energy&fuels

pubs.acs.org/EF Article

Investigating the Impact of Microporosity of Aminosilica Catalysts in Aldol Condensation Reactions for Biomass Upgrading of 5-Hydroxymethylfurfural and Furfuraldehyde to Fuels

Jee-Yee Chen and Nicholas A. Brunelli*

Cite This: *Energy Fuels* 2021, 35, 14885−14893 Read Online

ACCESS | Metrics & More | Article Recommendations | Supporting Information

ABSTRACT: Upgrading biomass to chemicals and fuels requires development of highly active and selective catalytic materials for important reactions such as the aldol condensation. The aldol condensation is a critical step to convert small molecules such as 5-hydroxymethylfurfural (HMF) and furfuraldehyde (FA) to larger complexes that can be used for fuels or chemicals. Whereas extensive work has examined aminosilica catalytic materials for aldol chemistry, these materials have received limited attention for HMF and FA conversion in spite of the capability of these materials to catalyze reactions in a cooperative manner. In this work, important structure−function relationships are investigated that demonstrate the impact of micropores in these materials. Materials are produced using a typical method (REG) and a method that produces limited to no micropores (NMP). The materials are grafted with aminosilanes and characterized using standard techniques. It is found that materials with limited to no micropores are more active for the aldol reaction and condensation for both FA with acetone and HMF with acetone. Additionally, the materials are tested in recycle experiments that showed the NMP catalyst retained higher activity after four catalytic cycles than the REG catalyst. Overall, the results have important implications for the design of materials for upgrading biomass into chemicals and fuels.

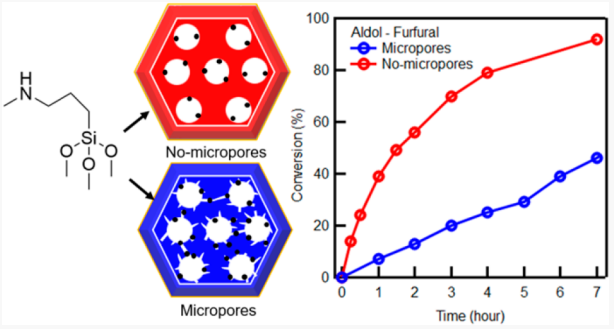

1. INTRODUCTION

Unlocking the potential of biomass as a source of fuel and chemicals requires identifying efficient and selective catalysts for upgrading the basic building blocks of plant matter.[1] A promising building block can be obtained through sequential hydrolysis, isomerization,[2−5] and dehydration[6−8] of the cellulose portion of the lignocellulosic biomass to produce 5-hydroxymethylfurfuraldehyde (HMF) and furfuraldehyde (FA). HMF and FA can subsequently be converted into polymer precursors,[9] feedstock chemicals,[10,11] and fuels.[12−14] One important upgrading route can involve coupling reactions such as aldol chemistry (i.e., reaction and condensation), as illustrated in Scheme 1. Aldol chemistry is a powerful method to upgrade small molecules provided that structure−function relationships can be elucidated that produce highly active catalysts.

Aldol chemistry can be catalyzed by a diverse array of catalysts, including homogeneous[15,16] and heterogeneous.[17−22] Homogeneous catalysts can either be a strong acid or a base, including organic amines.[23] Recent work has used sodium hydroxide to catalyze the reaction, resulting in efficient and rapid condensation of HMF and acetone.[12] Since homogeneous catalysts are difficult to separate, the development of heterogeneous catalysts would be beneficial. Many of these heterogeneous catalysts involve basic catalytic sites.[24−26] Whereas these materials are active and can catalyze the reaction through a base catalyzed mechanism, an intriguing alternative mechanism involves a cooperative interaction.[27,28] Cooperative interactions occur when two distinct moieties combine to produce a catalytic rate that is greater than the sum of the individual components. For aldol chemistry, cooperative interactions can be achieved between acid and base sites using materials such as aminosilica catalysts. The cooperative interactions of aminosilica materials can make it possible to produce highly active materials for biomass upgrading[32] that can operate at lower reaction temperatures than catalysts that are only basic or only acidic.

Aminosilica materials consist of an inorganic silica matrix and an organic amine tethered to the surface as an aminosilane. The proximity of the amine to the silica surface enables a low energy, cooperative reaction mechanism involving enamine formation (as shown in Scheme 2).[29] In the acid−base cooperative interaction, the amine can attack the ketone

Received: June 14, 2021
Revised: August 12, 2021
Published: August 25, 2021

https://doi.org/10.1021/acs.energyfuels.1c01934
Energy Fuels 2021, 35, 14885−14893

Scheme 1. Aldol Reaction and Condensation between Acetone and FA or Acetone and HMF to Produce the Keto-Alcohol or the Ene-One Product

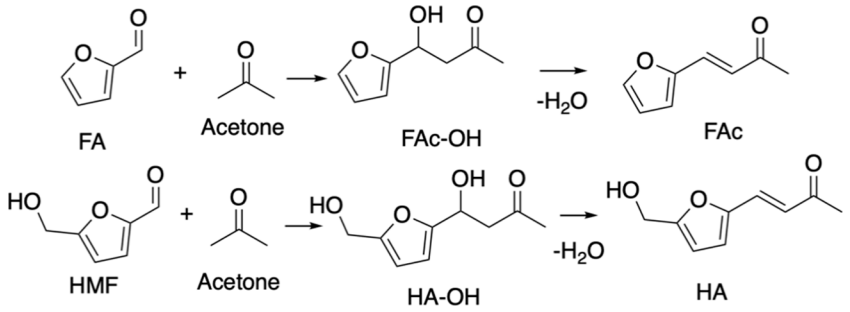

Scheme 2. Cooperative Reaction Mechanism of Aminosilica for Aldol Reaction and Condensation Involving Substrate Activation and Enamine Formation

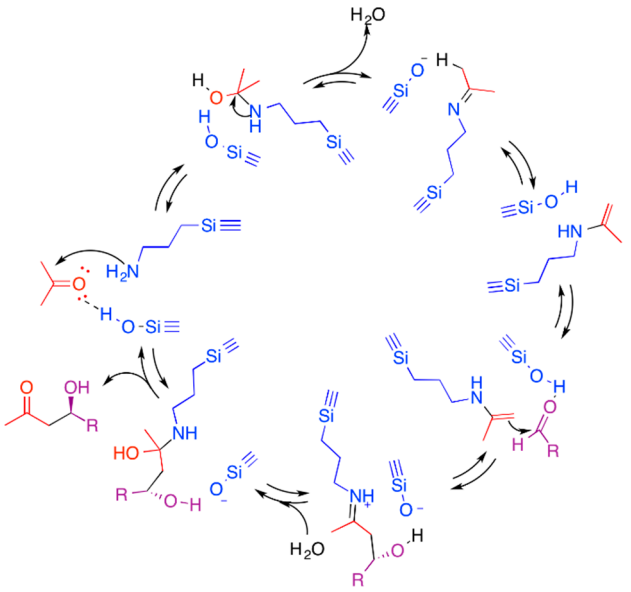

carbonyl to form the enamine intermediate that can attack the aldehyde carbonyl. The silanol group can serve to activate the oxygen of the ketone to lower the energy barrier for enamine formation to accelerate the reaction rate. This observation has been corroborated with spectroscopic[22] and computational work[30] investigating the reaction mechanism, and the mechanism has been demonstrated by computational work to be active for furanic substrates such as HMF and FA.[31] Currently, experimental work for aminosilica materials has focused on model reactions such as the coupling between 4-nitrobenzaldehyde and acetone rather than furanic compounds. Whereas direct experiments investigating furanic substrates would be valuable, these experimental observations for model compounds can provide valuable insights.

Experimental work investigating structure−function relationships of aminosilica materials have revealed several key elements that are beneficial for the aldol reaction. The aminosilane can have different features, including linker length,[33] amine type,[21] surface density,[34] and substituent size or structure.[35] The linker length should be a propyl linker so that the amine can act cooperatively with the surface silanols.[27] The cooperative interaction also requires accessible surface silanols, making it necessary to limit the surface density of the amine.[27] The amine can either be primary or secondary so that the enamine intermediate can be formed.[36] If limited water is present,[37] it has been found that secondary amines are more active than primary amines since the secondary amine reacting with the aldehyde substrate forms an unstable complex, whereas the aldehyde forms a stable complex that inhibits the reaction.[38,39] For secondary amines, a higher catalytic activity is obtained when the substituent is a methyl group since bulkier groups may limit the amine silanol interactions[2] or inhibit the reaction.[35]

Whereas the majority of research has focused on the structure of the aminosilane,[40,41] additional work has examined the effect of the silica support.[42] Indeed, it has been reported that the pore size of the silica support has minimal effect, but this observation was limited to the diameter range of 2.3 to 6.5 nm. Interestingly, common mesoporous materials such as SBA-15 also possess micropores.[43,44] Whereas previous work demonstrated the negative impact of micropores for the Knoevenagel condensation,[45] it is unclear how micropores may impact the catalytic properties of aminosilica materials for the aldol reaction and condensation of substrates relevant to biomass upgrading. It is possible to tune the amount of micropores in the material through adjusting the synthesis conditions.[46−48] Specifically, the amount of micropores in the material can be reduced through adjusting the hydrothermal temperature from the commonly used 100 °C to using a temperature of 130 °C.[44] Since the amount of micropores impacts the total surface area, it will be important to compare the catalytic materials at similar surface densities of amines to maintain a similar amount of surface silanols.[49] This is important because the surface density of aminosilanes has an impact on catalytic activity in different reactions, such as aldol reaction and condensation and Knoevenagel condensation. Indeed, the catalytic performance can be improved through using techniques such as low loading or bulky ligands that can create site isolated amines on the surface.[50,51] It is found that higher density of the organosilane interrupts the cooperative interaction between the organosilane and the silanol group on the surface. Hence, it is important to investigate the catalytic properties of materials that are functionalized with similar surface densities.

This work will investigate the impact of micropores on the catalytic activity for aminosilica materials in the aldol reaction and condensation. Initial work focuses on the synthesis of materials with conditions that are commonly used and with conditions that can reduce the total amount of micropores in the material. These materials are functionalized at a similar surface density with a secondary aminosilane. The materials are characterized using a battery of standard techniques, including nitrogen physisorption and elemental analysis. After character-

https://doi.org/10.1021/acs.energyfuels.1c01934
Energy Fuels 2021, 35, 14885−14893

ization, the materials will be tested in the aldol reaction and condensation using the combination of FA and acetone or HMF and acetone. The materials are further subjected to recycle experiments to investigate the stability of the catalytic materials. Overall, these studies will provide insights on the structure−function relationships involved in the design of catalytic materials for aldol chemistry relevant to upgrading biomass derived intermediates.

2. EXPERIMENTAL METHODS

2.1. Chemicals. The following chemicals are used as-received: tetraethyl orthosilicate (TEOS, 98%, Acros Organics), hydrochloric acid (HCl, 36.5−38.0% by wt., reagent grade, J. T. Baker), poly(ethylene glycol)-*block*-poly(propylene glycol)-*block*-poly-(ethylene glycol) (PEO-PPO-PEO, Pluronic P-123 (Sigma-Aldrich)), *N*-methylamino-3-propyl trimethoxysilane (Gelest), ethanol (200 Proof, anhydrous, 100 USP specs, Deconlabs), hexanes (ACS grade, Fisher chemical), toluene (ACS 101 grade, satisfies ASTM, Fisher chemicals), acetone (HPLC grade, J. T. Baker), 1,3,5-trimethylbenzene (Tokyo Chemical Industry), 2-furfuraldehyde (FA, 99%, Acros Organics), and 5-hydroxymethylfurfural (HMF, Ark Organic). Toluene (ACS grade, Macron Fine Chemicals) is dried using an MB-SPS DriSolv system (MBraun, Inc.).

2.2. Synthesis of SBA-15−Regular and Low Micropore. The mesoporous support SBA-15 is synthesized with limited to no micropore volume using a procedure previously reported.[3] Briefly, Pluronic P123 (2.89 g) is first dissolved in distilled water (76.7 mL) and hydrochloric acid (14.5 mL) with continuous stirring in an Erlenmeyer flask at 40°C. After the polymer is completely dissolved, TEOS (5.58 g) is added dropwise into the mixture and allowed to mix at 40°C for 24 h. This mixture is transferred to a Parr reactor without a stir bar and placed in an oven preheated to a high temperature for 24 h. For regular SBA-15 (REG-SBA-15), the high temperature is 100°C, whereas the high temperature is 130°C to produce the material with limited to no micropore (NMP-SBA-15). The Parr reactor is cooled to room temperature, and the mixture solution is filtered. The solids are washed with 800 mL of distilled water and dried in the oven overnight. After drying, the solids are calcined to remove the surfactant using a temperature program as follows: (1) increase from room temperature to 200°C at a ramp rate of 1.2°C min^{-1}, (2) maintain for 1 h, (3) increase to 550°C at a ramp rate of 1.2°C min^{-1}, (4) maintain for 4 h, and (5) cool back to room temperature.

2.3. Grafting Procedure. A gram of bare support silica is dried under reduced pressure (<20 mTorr) at 130°C for 15 h in a round-bottom flask. After degassing, the flask is attached to a Schlenk line for 30 min of degassing via purging with nitrogen flow through a septum. After purging with nitrogen, dry toluene (25 mL of toluene per 1 g of silica) is added into the flask and dispersed with stirring at 25°C. The organosilane (0.8 mmol of organosilane per 1 g of silica for NMP-SBA-15, 1.5 mmol of organolsilane per 1 g of silica for REG-SBA-15) is premixed with 10 mL of dry toluene and added dropwise to the silica mixture. The procedure and amount of the toluene added are the same for REG-SBA-15 and NMP -SBA-15, but the organosilane mixture reaction is slightly different (the mixture concentration for two materials is shown in Table S1). After 24 h, 20 μL of deionized water is injected into the mixture. The flask is then attached to a septum-sealed condenser, and the temperature is increased to 80°C under nitrogen purging. The purging is stopped once the mixture reaches 50°C and then maintained at 80°C for another 24 h with stirring. Later, the mixture is cooled to room temperature before filtration. The mixture is filtered, washing sequentially with 300 mL of toluene, 300 mL of pure hexane, and 300 mL of ethanol. The solids are dried under reduced pressure for 15 h.

2.4. Physical and Chemical Characterization. The materials are characterized using several standard techniques, including Thermogravimetric Analysis, elemental analysis, and nitrogen physisorption. Thermogravimetric Analysis (TGA) is performed using a Netzsch Jupiter STA 449 F5 from 20 to 900°C at a ramp rate of 10 K min^{-1} under the constant flow of nitrogen and air at 20 mL min^{-1} each. Nitrogen physisorption analysis is conducted using a Micromeritics Instrument (3Flex). Before analysis, the composite materials and bare SBA-15 are degassed for 24 h at 80°C. The Broekhoff−de Boer Frenkel−Halsey−Hill (BdB-FHH) method is applied for analyzing the average pore diameter distribution. The materials are analyzed for elemental composition (C, H, N) by Atlantic Microlab.

2.5. Catalytic Testing in Aldol Condensation and Reaction. A bulk solution is prepared that consists of 1,3,5-trimethylbenzene (40 mg, internal standard), acetone (10 mL), and 2-furfuraldehyde (96 mg) (Table S2). Using a micropipette, this solution (2 mL) is added to a 10 mL two-neck round-bottom flask with one of the necks sealed using a rubber septum. After transferring the solution, a small sample (50 μL) is withdrawn to serve as the t_0 sample. The secondary amine functionalized catalysts are then added to this mixture to obtain a 15 mol % amine loading (based on elemental analysis). The round-bottom flask is attached to a septum-sealed condenser under an active purge of nitrogen. The setup is then lowered into an oil bath preheated to the reaction temperature (50°C). The stirring speed is typically set to 600 rpm. Using a syringe equipped with a needle, samples (50 μL) are drawn periodically from the septum-sealed neck of the round-bottom flask. The nitrogen purge is switched to a static nitrogen environment after the 15-min sample is drawn. These samples are filtered using a plug of silica above a piece of cotton in glass pipettes. Samples are diluted using acetone before analyzing them on an Agilent 7820A GC-FID equipped with a Shimadzu SH-Rtx-5MS capillary column.

The catalytic testing procedure is similar for 5-hydroxymethylfurfural as a substrate in the aldol reaction and condensation with acetone. For HMF reactions, the bulk solution consists of 1,3,5-trimethylbenzene (40 mg, internal standard), acetone (10 mL), and 5-hydroxymethylfurfural (126 mg) (Table S3).

2.6. Catalyst Reuse Testing. The ability to reuse the catalyst is evaluated by testing the catalyst in a series of aldol reactions and condensations between FA and acetone. The first reaction is performed on a scale that is a factor of five larger than the single use catalyst testing to increase the amount of catalyst used to facilitate the recovery of the material for analysis and additional catalytic testing. The first catalytic testing is the same as the previous process with the exceptions that (1) a 25-mL two-neck round-bottom (RB) flask is used instead of a 10-mL RB flask and (2) 10 mL of the reaction mixture is used instead of 2 mL of the reaction mixture while maintaining a 15 mol % catalyst. After collecting data points over a 7-h period, the reaction mixture is quenched by removing the RB flask from the heated oil bath. The reaction mixture is filtered and washed with ethyl acetate (1 L). The solids are dried under reduced pressure for 15 h at 80°C. The dry material is characterized by nitrogen physisorption and elemental analysis. The remaining catalyst is used for another 7-h aldol reaction and condensation between 5-furfuraldehyde (FA) and acetone to check the catalytic activity change after using the catalyst for first, second, and third cycles. The recycle tests are performed using an amount of catalyst that corresponds to 15 mol % of amine, as determined by the elemental analysis result for the fresh catalyst.

3. RESULTS AND DISCUSSION

3.1. Catalyst Synthesis and Characterization. The demonstration of the successful synthesis of aminosilica catalytic materials is achieved using a series of steps involving support synthesis, postsynthetic grafting, and material characterization. The bare silica support is produced through the typical hydrothermal method to produce SBA-15. This includes a low temperature hydrolysis step at 40°C followed by a high temperature condensation step at 100°C. After separating the product from the synthesis solution, the material is calcined to produce a bare silica support that is referred to as REG-SBA-15.

https://doi.org/10.1021/acs.energyfuels.1c01934
Energy Fuels 2021, 35, 14885−14893

Table 1. Comparison of the Material Characteristics for the Catalytic Materials

material	BET surface area (m^2/g)[a]	micropore area (m^2/g)[a]	micropore volume (cm^3/g)[a]	pore diameter (nm)[b]	N content (wt %)[c]	surface density ($\mu mol/m^2$)
REG-SBA-15	950	180	0.072	6.8		
REG-SBA-15-2°Am	510	0	0	6.3	1.88	1.41
NMP-SBA-15	520	72	0.023	8.8		
NMP-SBA-15-2°Am	490	11	0	8.9	0.96	1.31

[a]Calcuated from the nitrogen physisorption adsorption isotherm. [b]Calculated using the BdB-FHH method. [c]From elemental analysis.

REG-SBA-15 is characterized at the different stages of synthesis using a battery of standard methods, including N_2 physisorption, Thermogravimetric Analysis (TGA), and elemental analysis. First, the material is analyzed with N_2 physisorption to investigate the textural properties, including the surface area (950 m^2/g), as listed in Table 1. The physisorption isotherm result for the NMP SBA-15 is type IV with a hysteresis loop that is type H1. The isotherm is consistent with a material having mesopores and has similar properties to previous syntheses.[2] The isotherm is further analyzed using the BdB-FHH model[52] to determine the pore size from the adsorption isotherm. The pore size is calculated to be 6.8 nm (Figure S1), which is similar to previous work. Interestingly, the material is determined to also have micropores with the t-plot analysis indicating that the material has a micropore volume of 0.072 cm^3/g and a micropore surface area of 180 m^2/g. The micropore surface area corresponds to ~20% of the total surface area for organosilane functionalization.

REG-SBA-15 is functionalized with an *N*-methylamino-3-propyl trimethoxysilane to produce a secondary aminosilica composite catalyst. The functionalized material is characterized with TGA, nitrogen physisorption, and elemental analysis (shown in Figure 1). After the grafting procedure, TGA has a mass loss (~10 wt %) in the range of 250−550°C that is consistent with organic functionalization, as shown in Figure S2. The nitrogen physisorption isotherm for REG-SBA-15-2°Am is type IV with an H1 hysteresis. From BdB-FHH analysis of the adsorption isotherm, the pore size is determined to be 6.3 nm, which is similar to REG-SBA-15. The is consistent with the grafting procedure being sufficiently mild to prevent material degradation. At the same time, it is observed that the micropore area and micropore volume are reduced or even eliminated during the grafting procedure. This suggests that a portion of the organosilanes may be grafting in the micropores of the material. Since potential upgrading reactions for biomass compounds may produce large products, the grafting of the aminosilane in the micropores may be problematic. Whereas the size of the mesopores has been shown to have limited to no impact on catalytic activity,[34] the impact of micropores on the catalytic activity for aldol reaction and condensation of biomass derived furanics has not been rigorously investigated.

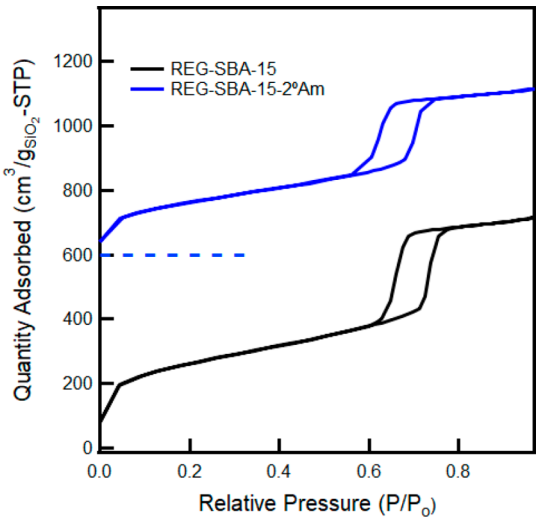

Figure 1. Comparison of nitrogen physisorption isotherm for REG-SBA-15 and REG-SBA-15-2°Am. The data for REG-SBA-15-2°Am is offset on the *y*-axis by 600 for clarity. A dashed line is included at this offset location.

The impact of micropores on catalytic activity can be investigated through synthesizing a bare material with limited to no micropores. Prior work indicates that modifying the synthesis conditions of SBA-15 through increasing the temperature of the hydrothermal step to 130°C produces a material that would have limited to no micropores,[44] leading to the naming convention NMP-SBA-15. NMP-SBA-15 is characterized using nitrogen physisorption, resulting in a type IV isotherm with an H1 hysteresis. Analysis of the isotherm data reveals that the modification in the synthesis procedure reduces the micropore surface area and volume by a factor of 3 to 72 m^2/g and 0.023 cm^3/g, consistent with expectations. One important aspect to note is that BdB-FHH analysis of the adsorption isotherm indicates that the pore size for NMP-SBA-15 is 8.8 nm (Figure S3). Since previous work has demonstrated that the aldol chemistry does not have a dependence on the pore size,[34] REG-SBA-15 and NMP-SBA-15 can be used to investigate the effect of micropores on the catalytic activity for the aldol reaction and condensation.

The NMP-SBA-15 material is subjected to the grafting procedure. Importantly, aldol chemistry is known to benefit from cooperative interactions of surface immobilized amines. Since the quantity of surface density of silanols for bare silica materials is approximately constant, the NMP-SBA-15 material is functionalized with the target of achieving a similar surface density of amines as REG-SBA-15-2°Am. From elemental analysis and the surface area of the bare support, the surface density of amines on REG-SBA-15-2°Am is determined to be 1.41 $\mu mol/m^2$. With this surface density as a target, NMP-SBA-15 is grafted with the aminosilane at different concentrations until achieving a material with a comparable surface density of 1.31 $\mu mol/m^2$. TGA corroborates the organic loading, as shown in Figure S4. The resulting material is labeled NMP-SBA-15-2°Am.

NMP-SBA-15-2°Am is also characterized using nitrogen physisorption. As shown in Figure 2, the resulting isotherm remains type IV, indicating the material contains mesopores.

https://doi.org/10.1021/acs.energyfuels.1c01934
Energy Fuels 2021, 35, 14885−14893

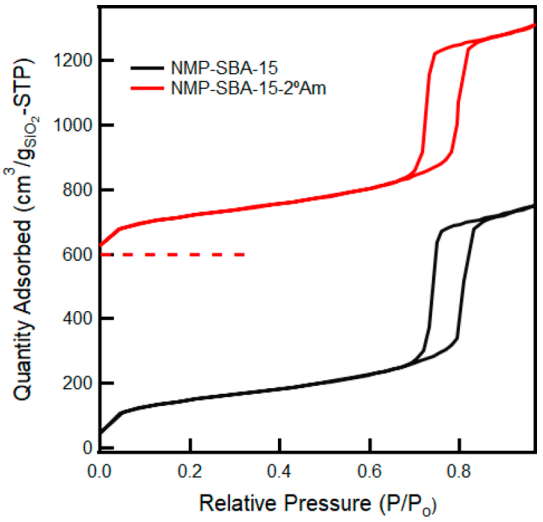

Figure 2. Comparison of nitrogen physisorption isotherm for NMP-SBA-15 and NMP-SBA-15-2°Am. The data for NMP-SBA-15-2°Am is offset on the *y*-axis by 600 for clarity. A dashed line is included at this offset location.

NMP-SBA-15-2°Am has less micropore surface area and pore volume compared to the bare silica NMP-SBA-15. This suggests that a portion of the aminosilane grafts into the micropores of the support. Since NMP-SBA-15 has less micropore volume and surface area before grafting, the expectation is that NMP-SBA-15-2°Am would have a greater fraction of the aminosilanes located in the mesopores compared to REG-SBA-15-2°Am. Therefore, differences in catalytic activity would reflect the impact of micropores.

3.2. Catalytic Testing. Initial catalytic work focuses on testing the materials for catalytic activity in the aldol reaction and condensation between 2-furfuraldehyde (FA) and acetone. The reaction is performed using an excess of acetone, making it possible to focus on the progress of the single aldol C−C bond forming process rather than the potential double aldol condensation. At the same time, the excess of acetone means that the reaction progress can be monitored through calculating the conversion of FA over time. As shown in Figure 3, the conversion of FA increases with time, reaching a conversion of ∼55% in 7 h.

For comparison, NMP-SBA-15-2°Am is also tested for catalytic activity in the same reaction. For both REG-SBA-15-2°Am and NMP-SBA-15-2°Am, the amount of catalyst is adjusted to achieve a mole percentage of catalyst of 15% N based on elemental analysis of the FA in the reaction solution. Even though the reaction mixtures have the same amount of amine added, it is determined that NMP-SBA-15-2°Am achieves >90% conversion in 7 h, which is a FA conversion greater than the conversion achieved with REG-SBA-15-2°Am. Using the conversion data, the reaction rate constant is calculated using a first order kinetic model. For the reaction converting FA, it is determined that the rate constant for REG-SBA-15-2°Am is 0.19 h^{-1}, whereas for NMP-SBA-15-2°Am, it is 0.44 h^{-1}, as listed in Table 2. The reaction rate constants when converting FA differ by a factor of 2. The observed difference suggests that the two materials either have different types of sites or a different fraction of sites that are active. Future work is aimed at differentiating between these two different scenarios, which is beyond the scope of the current work.

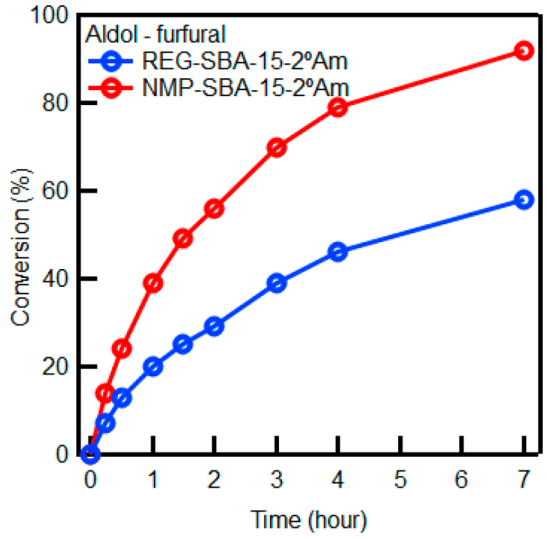

Figure 3. Comparison of the conversion of FA over time in the aldol reaction and condensation as catalyzed by REG-SBA-15-2°Am and NMP-SBA-15-2°Am. The reaction conditions include the following: 15 mol % N, 50°C, and 1 mM furfural in acetone with a stir rate of 600 rpm.

Table 2. Comparison of the First Order Rate Constant for the Different Catalysts When Converting Either FA or HMF

material	k_{FA} (h^{-1})	k_{HMF} (h^{-1})
REG-SBA-15-2°Am	0.19	0.31
NMP-SBA-15-2°Am	0.44	0.50

In addition to the aldol chemistry with FA, it is possible to use the product HMF processed through aldol condensation as a possible source of fuel or chemicals.[53] Therefore, the conversion over time for the two materials is investigated using HMF as a substrate in the aldol reaction and condensation with acetone, as shown in Figure 4. In the same 7 h time interval, REG-SBA-15-2°Am is able to achieve approximately

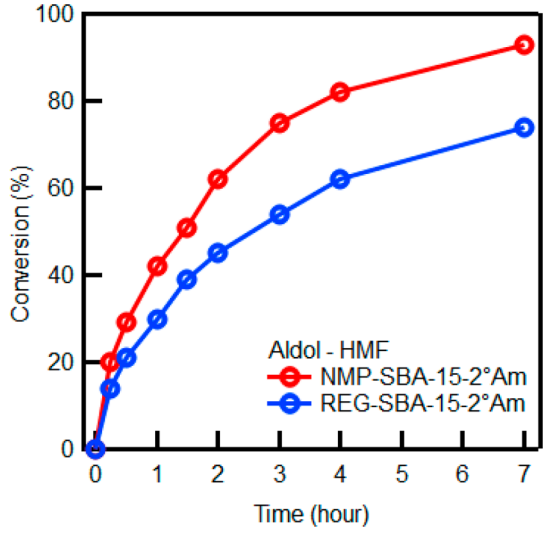

Figure 4. Comparison of the conversion of HMF over time in the aldol reaction and condensation as catalyzed by REG-SBA-15-2°Am and NMP-SBA-15-2°Am. The reaction conditions include the following: 15 mol % N, 50°C, and 1 mM HMF in acetone with a stir rate of 600 rpm.

https://doi.org/10.1021/acs.energyfuels.1c01934
Energy Fuels 2021, 35, 14885−14893

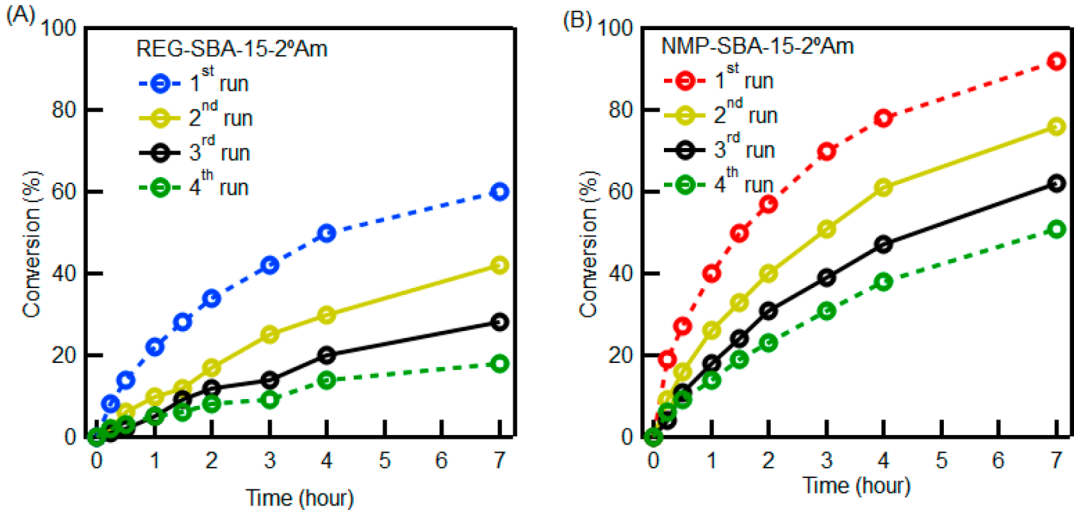

Figure 5. Comparison of the conversion of FA over time in the aldol reaction and condensation as catalyzed by (A) REG-SBA-15-2°Am or (B) NMP-SBA-15-2°Am for a different number of reaction cycles. The reaction conditions include the following: 15 mol % N, 50°C, and 1 mM FA in acetone with a stir rate of 600 rpm. The dashed lines are the catalytic testing based on the elemental analysis result.

60% conversion of HMF, whereas NMP-SBA-15-2°Am can achieve >90% conversion of HMF. Consistent with the experiments with FA, the catalytic activity of NMP-SBA-15-2°Am is higher than REG-SBA-15-2°Am. The reaction rate constant is calculated for REG-SBA-15-2°Am to be 0.31 h^{-1}, whereas for NMP-SBA-15-2°Am, it is 0.50 h^{-1}. Interestingly, the reaction rate constants for HMF are greater than the reaction rate constants for FA. Yet, the difference in reaction rate constants for HMF between the two catalysts is smaller than the difference in reaction rate constants for FA. This suggests a subtle complexity to these materials in that the fraction and/or type of active site is influenced by the structure of the substrate. Overall, these combined studies demonstrate the impact of micropores in aminosilica materials on aldol chemistry for substrates relevant for biomass upgrading.

3.3. Reuse Catalyst Testing. The catalyst stability is evaluated through reusing the catalyst in a series of reactions. As shown in Figure 5A, REG-SBA-15-2°Am achieves an FA conversion of 60% at 7 h. The conversion over time data are used to calculate a rate constant of 0.216 h^{-1}, as listed in Table 3. The catalyst is filtered from the reaction mixture and washed with ethyl acetate (1 L). After washing, the material is dried under reduced pressure (<10 mTorr) for 15 h before a second catalytic test. For the second and third catalytic tests, the catalyst is able to convert FA, but the activity decreases for each round of catalyst reuse, resulting in rate constants of 0.093 h^{-1} and 0.061 h^{-1} for the second and third cycles, respectively. For the third cycle, the catalytic activity is reduced to 28% of its original catalytic activity (k/k_1, where k is the rate constant and k_1 is the rate constant of the first use of the catalyst), representing a substantial loss in activity.

Table 3. Comparison of the Reused Catalyst Activity for the First Order Rate Constant for the Different Reuse Cycles When Converting FA

		conversion at 7 h (%)	k	k/k_1
NMP-SBA-15-2°Am	first run	92	0.456	
	second run	76	0.269	0.59
	third run	62	0.188	0.41
	fourth run	51	0.139	0.31
REG-SBA-15-2°Am	first run	60	0.216	
	second run	42	0.093	0.43
	third run	28	0.061	0.28
	fourth run	18	0.043	0.2

The observed reduction in catalytic activity could occur by several potential mechanisms, including degradation of the material mesopore structure or leaching of the organosilane that would manifest as a reduction in nitrogen content. After the third catalytic cycle, the material is analyzed with nitrogen physisorption and elemental analysis. Nitrogen physisorption of the material (REG-SBA-15-2°Am) after each cycle reveals that the material BET surface area reduces from 510 m^2/g to 360 m^2/g (after 1 cycle) to 360 m^2/g (after 2 cycles) to 340 m^2/g (Table S4). Whereas the reduction in pore size after the first cycle could be responsible for the observed decrease in catalyst activity, the catalyst continues to lose activity with each cycle, but the BET surface area remains relatively constant after the first catalyst use, suggesting that other mechanisms could be responsible for loss of catalytic activity (Figure S5). In addition, elemental analysis demonstrates that the nitrogen content reduces slightly from 1.88 to 1.73 wt % N (after three cycles), which corresponds to an 8% reduction in N content. The slight reduction in nitrogen content is inconsistent with the 72% loss of catalytic activity. The elemental analysis data are used to adjust the amount of catalyst used for the fourth catalytic cycle, which shows a further reduction in catalytic activity. This suggests that organosilane leaching is not a predominant mechanism for catalyst deactivation. Whereas the N content remains relatively constant, elemental analysis reveals that the C wt % increases. This suggests that organic species could accumulate in the material. Interestingly, the material changes color with each catalytic cycle, as shown in Figure S7. With each additional cycle, the material turns a darker shade of brown. Similar discoloration has been observed for aminosilica materials tested in the aldol reaction and condensation,[54] suggesting that catalyst deactivation is caused by accumulation of organic species in the materials.

For comparison, NMP-SBA-15-2°Am is also evaluated for reusability in the aldol reaction and condensation of FA and acetone. As is shown in Figure 5B, the catalytic activity of

https://doi.org/10.1021/acs.energyfuels.1c01934
Energy Fuels 2021, 35, 14885−14893

NMP-SBA-15-2°Am decreased with each reuse of the catalyst. Calculating the reaction rate constant, NMP-SBA-15-2°Am has greater activity than REG-SBA-15-2°Am that has been through the same number of catalytic cycles. In addition, NMP-SBA-15-2°Am retains a greater fraction of its original catalytic activity than REG-SBA-15-2°Am.

These results for NMP-SBA-15-2°Am are promising, but similar trends in the characterization data of the recovered catalysts are observed. First, nitrogen physisorption measurements indicate that NMP-SBA-15-2°Am loses surface area after the first cycle, reducing from 490 m^2/g to ~390 m^2/g (Table S5) and remaining approximately constant even after three more cycles (Figure S6). Elemental analysis indicates that the nitrogen content remains approximately constant at 0.96 wt % for the fresh material and the material after three catalytic cycles, indicating that organosilane leaching is not occurring to a measurable extent. The N content from elemental analysis is used to calculate the amount of catalyst to be added for the fourth cycle to achieve a 15 mol % loading (Table 4). The catalytic activity for the fourth catalytic cycle is lower than the catalytic activity for the third catalytic cycle. As observed with REG-SBA-15-2°Am, the C wt % increases, consistent with organic accumulation in the material. It is also observed that the material becomes brown (Figure S7). After the same number of cycles, NMP-SBA-15-2°Am is less brown, and there is less organic accumulation than with REG-SBA-15-2°Am. These results illustrate that the deactivation mechanism of the two materials is likely similar. Yet, NMP-SBA-15-2°Am has shown to be a more stable catalyst than REG-SBA-15-2°Am.

Table 4. Comparison of the Fresh Catalyst and Third Time Reused Catalyst for Elemental Analysis Result

material	number of cycles	C (wt %)	N (wt %)
REG-SBA-15-2°Am	initial	7.57	1.88
	after third run	11.62	1.73
NMP-SBA-15-2°Am	initial	4.26	0.96
	after third run	6.8	0.96

4. SUMMARY

The impact of micropores on catalytic activity of aminosilica materials is investigated through grafting aminosilanes onto SBA-15 supports that are produced using conventional methods (REG-SBA-15) and a modified method that results in limited to no micropore volume and surface area (NMP-SBA-15). The grafting procedure is used to create two catalysts with similar surface density. From catalytic testing, it is observed that NMP-SBA-15 materials are more active and more stable catalysts than REG-SBA-15 materials. The differences in catalytic activity are influenced by the substrates involved in the reaction. Overall, the work demonstrates that tuning the structure of the material support can impact the ability of the material to catalyze these important reactions for upgrading biomass.

■ ASSOCIATED CONTENT

Supporting Information

The Supporting Information is available free of charge at https://pubs.acs.org/doi/10.1021/acs.energyfuels.1c01934.

Information regarding material characterization data, tables of catalytic data, and additional experimental details (PDF)

■ AUTHOR INFORMATION

Corresponding Author

Nicholas A. Brunelli − *William G. Lowrie Department of Chemical and Biomolecular Engineering, The Ohio State University, Columbus, Ohio 43210, United States;* orcid.org/0000-0003-0712-8966; Email: brunelli.2@osu.edu

Author

Jee-Yee Chen − *William G. Lowrie Department of Chemical and Biomolecular Engineering, The Ohio State University, Columbus, Ohio 43210, United States*

Complete contact information is available at: https://pubs.acs.org/10.1021/acs.energyfuels.1c01934

Notes

The authors declare no competing financial interest.

■ ACKNOWLEDGMENTS

This work was supported by the National Science Foundation (NSF CBET 2015669).

■ REFERENCES

(1) Wettstein, S. G.; Martin Alonso, D.; Gurbuz, E. I.; Dumesic, J. A. A Roadmap for Conversion of Lignocellulosic Biomass to Chemicals and Fuels. *Curr. Opin. Chem. Eng.* **2012**, *1* (3), 218−224.

(2) Deshpande, N.; Cho, E. H.; Spanos, A. P.; Lin, L.-C.; Brunelli, N. A. Tuning Molecular Structure of Tertiary Amine Catalysts for Glucose Isomerization. *J. Catal.* **2019**, *372*, 119−127.

(3) Deshpande, N.; Pattanaik, L.; Whitaker, M. R.; Yang, C.-T.; Lin, L.-C.; Brunelli, N. A. Selectively Converting Glucose to Fructose Using Immobilized Tertiary Amines. *J. Catal.* **2017**, *353*, 205−210.

(4) Moliner, M.; Román-Leshkov, Y.; Davis, M. E. Tin-Containing Zeolites Are Highly Active Catalysts for the Isomerization of Glucose in Water. *Proc. Natl. Acad. Sci. U. S. A.* **2010**, *107* (14), 6164−6168.

(5) Bhosale, S. H.; Rao, M. B.; Deshpande, V. V. Molecular and Industrial Aspects of Glucose Isomerase. *Microbiol. Rev.* **1996**, *60* (2), 280−300.

(6) Whitaker, M. R.; Parulkar, A.; Brunelli, N. A. Selective Production of 5-Hydroxymethylfurfural from Fructose in the Presence of an Acid-Functionalized SBA-15 Catalyst Modified with a Sulfoxide PolymerSyst. *Des. Eng.* **2020**, *5*, 257.

(7) Munavu, R. M.; Musau, R. M. The Preparation of 5-Hydroxymethyi-2-Furaldehyde (HMF) from D-Fructose in the Presence of DMSO. *Biomass* **1987**, *13*, 67−74.

(8) Román-Leshkov, Y.; Chheda, J. N.; Dumesic, J. A. Production of Hydroxymethylfurfural from Fructose. *Science (Washington, DC, U. S.)* **2006**, *312* (4), 1933−1937.

(9) Chang, H.; Gilcher, E. B.; Huber, G. W.; Dumesic, J. A. Synthesis of Performance-Advantaged Polyurethanes and Polyesters from Biomass-Derived Monomers by Aldol-Condensation of 5-Hydroxymethyl Furfural and Hydrogenation. *Green Chem.* **2021**, *23*, 4355.

(10) Mittal, A.; Pilath, H. M.; Johnson, D. K. Direct Conversion of Biomass Carbohydrates to Platform Chemicals: 5-Hydroxymethylfurfural (HMF) and Furfural. *Energy Fuels* **2020**, *34* (3), 3284−3293.

(11) Taarning, E.; Nielsen, I. S.; Egeblad, K.; Madsen, R.; Christensen, C. H. Chemicals from Renewables: Aerobic Oxidation of Furfural and Hydroxymethylfurfural over Gold Catalysts. *ChemSusChem* **2008**, *1* (1−2), 75−78.

(12) Chang, H.; Huber, G. W.; Dumesic, J. A. Synthesis of Biomass-Derived Feedstocks for the Polymers and Fuels Industries from 5-

(Hydroxymethyl)Furfural (HMF) and Acetone. *Green Chem.* **2019**, *21*, 5532.
(13) Su, M.; Li, W.; Zhang, T.; Xin, H. S.; Li, S.; Fan, W.; Ma, L. Production of Liquid Fuel Intermediates from Furfural via Aldol Condensation over Lewis Acid Zeolite Catalysts. *Catal. Sci. Technol.* **2017**, *7* (16), 3555−3561.
(14) Climent, M. J.; Corma, A.; Iborra, S. Conversion of Biomass Platform Molecules into Fuel Additives and Liquid Hydrocarbon Fuels. *Green Chem.* **2014**, *16* (2), 516−547.
(15) List, B.; Lerner, R. A.; Barbas III, C. F. Proline-Catalyzed Direct Asymmetric Aldol Reactions. *J. Am. Chem. Soc.* **2000**, *122* (10), 2395−2396.
(16) Gutsche, C. D.; Buriks, R. S.; Nowotny, K.; Grassner, H. Tertiary Amine Catalysis of the Aldol Condensation. *J. Am. Chem. Soc.* **1962**, *84* (3), 3775−3777.
(17) Kubota, Y.; Goto, K.; Miyata, S.; Goto, Y.; Fukushima, Y.; Sugi, Y. Enhanced Effect of Mesoporous Silica on Base-Catalyzed Aldol Reaction. *Chem. Lett.* **2003**, *32* (3), 234−235.
(18) Bass, J. D.; Anderson, S. L.; Katz, A. The Effect of Outer-Sphere Acidity on Chemical Reactivity in a Synthetic Heterogeneous Base Catalyst. *Angew. Chem.* **2003**, *115* (42), 5377−5380.
(19) Bass, J. D.; Solovyov, A.; Pascall, A. J.; Katz, A. Acid-Base Bifunctional and Dielectric Outer-Sphere Effects in Heterogeneous Catalysis: A Comparative Investigation of Model Primary Amine Catalysts. *J. Am. Chem. Soc.* **2006**, *128*, 3737.
(20) Kubota, Y.; Yamaguchi, H.; Yamada, T.; Inagaki, S.; Sugi, Y.; Tatsumi, T. Further Investigations on the Promoting Effect of Mesoporous Silica on Base-Catalyzed Aldol Reaction. *Top. Catal.* **2010**, *53* (7−10), 492−499.
(21) Kandel, K.; Althaus, S. M.; Peeraphatdit, C.; Kobayashi, T.; Trewyn, B. G.; Pruski, M.; Slowing, I. I. Substrate Inhibition in the Heterogeneous Catalyzed Aldol Condensation: A Mechanistic Study of Supported Organocatalysts. *J. Catal.* **2012**, *291*, 63−68.
(22) Kandel, K.; Althaus, S. M.; Peeraphatdit, C.; Kobayashi, T.; Trewyn, B. G.; Pruski, M.; Slowing, I. I. Solvent-Induced Reversal of Activities between Two Closely Related Heterogeneous Catalysts in the Aldol Reaction. *ACS Catal.* **2013**, *3* (2), 265−271.
(23) Bender, T. A.; Dabrowski, J. A.; Gagné, M. R. Homogeneous Catalysis for the Production of Low-Vol., High-Value Chemicals from Biomass. *Nat. Rev. Chem.* **2018**, *2*, 35.
(24) Kikhtyanin, O.; Kelbichová, V.; Vitvarová, D.; Kubů, M.; Kubička, D. Aldol Condensation of Furfural and Acetone on Zeolites. *Catal. Today* **2014**, *227*, 154−162.
(25) O'Neill, R. E.; Vanoye, L.; De Bellefon, C.; Aiouache, F. Aldol-Condensation of Furfural by Activated Dolomite Catalyst. *Appl. Catal., B* **2014**, *144* (1), 46−56.
(26) Sosa, N.; Chanlek, N.; Wittayakun, J. Facile Ultrasound-Assisted Grafting of Silica Gel by Aminopropyltriethoxysilane for Aldol Condensation of Furfural and Acetone. *Ultrason. Sonochem.* **2020**, *62*, 104857.
(27) Brunelli, N. A.; Jones, C. W. Tuning Acid-Base Cooperativity to Create next Generation Silica-Supported Organocatalysts. *J. Catal.* **2013**, *308*, 60−72.
(28) Lauwaert, J.; Moschetta, E. G.; Van Der Voort, P.; Thybaut, J. W.; Jones, C. W.; Marin, G. B. Spatial Arrangement and Acid Strength Effects on Acid-Base Cooperatively Catalyzed Aldol Condensation on Aminosilica Materials. *J. Catal.* **2015**, *325*, 19−25.
(29) Zeidan, R. K.; Davis, M. E. The Effect of Acid-Base Pairing on Catalysis: An Efficient Acid−Base Functionalized Catalyst for Aldol Condensation. *J. Catal.* **2007**, *247*, 379−382.
(30) Kim, K. C.; Moschetta, E. G.; Jones, C. W.; Jang, S. S. Molecular Dynamics Simulations of Aldol Condensation Catalyzed by Alkylamine-Functionalized Crystalline Silica Surfaces. *J. Am. Chem. Soc.* **2016**, *138* (24), 7664−7672.
(31) Zhang, J. F.; Wang, Z. M.; Lyu, Y. J.; Xie, H.; Qi, T.; Si, Z. B.; Liu, L. J.; Yang, H. Q.; Hu, C. W. Synergistic Catalytic Mechanism of Acidic Silanol and Basic Alkylamine Bifunctional Groups over SBA-15 Zeolite toward Aldol Condensation. *J. Phys. Chem. C* **2019**, *123* (8), 4903−4913.
(32) Shylesh, S.; Gokhale, A. A.; Ho, C. R.; Bell, A. T. Novel Strategies for the Production of Fuels, Lubricants, and Chemicals from Biomass. *Acc. Chem. Res.* **2017**, *50* (10), 2589−2597.
(33) Brunelli, N. A.; Didas, S. A.; Venkatasubbaiah, K.; Jones, C. W. Tuning Cooperativity by Controlling the Linker Length of Silica-Supported Amines in Catalysis and CO 2 Capture. *J. Am. Chem. Soc.* **2012**, *134* (34), 13950−13953.
(34) Brunelli, N. A.; Jones, C. W. Tuning Acid−Base Cooperativity to Create next Generation Silica-Supported Organocatalysts. *J. Catal.* **2013**, *308*, 60−72.
(35) Lauwaert, J.; De Canck, E.; Esquivel, D.; Van Der Voort, P.; Thybaut, J. W.; Marin, G. B. Effects of Amine Structure and Base Strength on AcidCatal. *Catal. Today* **2015**, *246*, 35−45.
(36) Bahmanyar, S.; Houk, K. N. Transition States of Amine-Catalyzed Aldol Reactions Involving Enamine Intermediates-Theoretical Studies of Mechanism, Reactivity, and Stereoselectivity. *J. Am. Chem. Soc.* **2001**, *123* (45), 11273−11283.
(37) Singappuli-Arachchige, D.; Kobayashi, T.; Wang, Z.; Burkhow, S. J.; Smith, E. A.; Pruski, M.; Slowing, I. I. Interfacial Control of Catalytic Activity in the Aldol Condensation: Combining the Effects of Hydrophobic Environments and Water. *ACS Catal.* **2019**, *9* (6), 5574−5582.
(38) Shylesh, S.; Hanna, D.; Gomes, J.; Canlas, C. G.; Head-Gordon, M.; Bell, A. T. The Role of Hydroxyl Group Acidity on the Activity of Silica-Supported Secondary Amines for the Self-Condensation of n-Butanal. *ChemSusChem* **2015**, *8* (3), 466−472.
(39) Shylesh, S.; Hanna, D.; Gomes, J.; Krishna, S.; Canlas, C. G.; Head-Gordon, M.; Bell, A. T. Tailoring the Cooperative Acid-Base Effects in Silica-Supported Amine Catalysts: Applications in the Continuous Gas-Phase Self-Condensation of n -Butanal. *ChemCatChem* **2014**, *6*, 1283−1290.
(40) Lauwaert, J.; Moschetta, E. G.; Van Der Voort, P.; Thybaut, J. W.; Jones, C. W.; Marin, G. B. Spatial Arrangement and Acid Strength Effects on Acid−Base Cooperatively Catalyzed Aldol Condensation on Aminosilica Materials. *J. Catal.* **2015**, *325*, 19−25.
(41) Chen, H.-T.; Trewyn, B. G.; Wiench, J. W.; Pruski, M.; Lin, V. S.-Y. Urea and Thiourea-Functionalized Mesoporous Silica Nanoparticle Catalysts with Enhanced Catalytic Activity for Diels-Alder Reaction. *Top. Catal.* **2010**, *53*, 187−191.
(42) Moschetta, E. G.; Brunelli, N. A.; Jones, C. W. Reaction-Dependent Heteroatom Modification of Acid-Base Catalytic Cooperativity in Aminosilica Materials. *Appl. Catal., A* **2015**, *504*, 429−439.
(43) Pollock, R. A.; Walsh, B. R.; Fry, J.; Ghampson, I. T.; Melnichenko, Y. B.; Kaiser, H.; Pynn, R.; Desisto, W. J.; Wheeler, M. C.; Frederick, B. G. Size and Spatial Distribution of Micropores in SBA-15 Using CM-SANS. *Chem. Mater.* **2011**, *23* (17), 3828−3840.
(44) Galarneau, A.; Renzo, F. Di. True Microporosity and Surface Area of Mesoporous SBA-15 Silicas as a Function of Synthesis Temperature. *Langmuir* **2001**, *17*, 8328−8335.
(45) Kane, A.; Deshpande, N.; Brunelli, N. A. Impact of Surface Loading on Catalytic Activity of Regular and Low Micropore SBA-15 in the Knoevenagel Condensation. *AIChE J.* **2019**, *65* (12), e16791.
(46) Kruk, M.; Jaroniec, M.; Ko, C. H.; Ryoo, R. Characterization of the Porous Structure of SBA-15. *Chem. Mater.* **2000**, *12* (7), 1961−1968.
(47) Flodström, K.; Alfredsson, V. Influence of the Block Length of Triblock Copolymers on the Formation of Mesoporous Silica. *Microporous Mesoporous Mater.* **2003**, *59* (2−3), 167−176.
(48) Singh, S.; Kumar, R.; Setiabudi, H. D.; Nanda, S.; Vo, D. V. N. Advanced Synthesis Strategies of Mesoporous SBA-15 Supported Catalysts for Catalytic Reforming Applications: A State-of-the-Art Review. *Appl. Catal., A* **2018**, *559*, 57.
(49) Lauwaert, J.; De Canck, E.; Esquivel, D.; Thybaut, J. W.; Van Der Voort, P.; Marin, G. B. Silanol-Assisted Aldol Condensation on Aminated Silica: Understanding the Arrangement of Functional Groups. *ChemCatChem* **2014**, *6*, 255−264.
(50) Sharma, K. K.; Buckley, R. P.; Asefa, T. Optimizing Acid-Base Bifunctional Mesoporous Catalysts for the Henry Reaction: Effects of

https://doi.org/10.1021/acs.energyfuels.1c01934
Energy Fuels 2021, 35, 14885−14893

the Surface Density and Site Isolation of Functional Groups. *Langmuir* **2008**, *24* (24), 14306−14320.
(51) Hicks, J. C.; Jones, C. W. Controlling the Density of Amine Sites on Silica Surfaces Using Benzyl Spacers. *Langmuir* **2006**, *22* (6), 2676−2681.
(52) Schmidt-Winkel, P.; Lukens, W. W.; Zhao, D.; Yang, P.; Chmelka, B. F.; Stucky, G. D. Mesocellular Siliceous Foams with Uniformly Sized Cells and Windows [5]. *J. Am. Chem. Soc.* **1999**, *121* (1), 254−255.
(53) West, R. M.; Liu, Z. Y.; Peter, M.; Gärtner, C. A.; Dumesic, J. A. Carbon-Carbon Bond Formation for Biomass-Derived Furfurals and Ketones by Aldol Condensation in a Biphasic System. *J. Mol. Catal. A: Chem.* **2008**, *296* (1−2), 18−27.
(54) De Vylder, A.; Lauwaert, J.; De Clercq, J.; Van Der Voort, P.; Thybaut, J. W. The Effect of Water on the Reusability of Aminated Mesoporous Silica Catalysts for Aldol Condensations. *J. Catal.* **2018**, *361*, 51−61.

https://doi.org/10.1021/acs.energyfuels.1c01934
Energy Fuels 2021, 35, 14885−14893